

# Diode laser spectroscopy of methyl iodide at 850 nm

A. Lucchesini\*

*Istituto Nazionale di Ottica - CNR - S.S. "Adriano Gozzini"*

*Area della Ricerca - Pisa - Italy*

(Dated: April 12, 2023)

Using the Tunable Diode Laser Absorption Spectroscopy (TDLAS) 82  $\text{CH}_3\text{I}$  ro-vibrational overtone absorption were detected for the first time between  $11660$  and  $11840\text{ cm}^{-1}$  ( $844 - 857\text{ nm}$ ), with strengths estimated to be around  $10^{-27} - 10^{-26}\text{ cm}^2/\text{molecule}$ . The lines have been measured utilizing commercial heterostructure F-P type diode lasers, multipass cells and the wavelength modulation spectroscopy with second harmonic detection technique. A high modulation amplitude approach was adopted for the analysis of the line shapes. Self-broadening coefficients have been obtained for two lines.

## I. INTRODUCTION

This work on methyl iodide or iodomethane ( $\text{CH}_3\text{I}$ ) is the natural continuation of the previous ones on methyl halides  $\text{CH}_3\text{F}$  [1] and  $\text{CH}_3\text{Cl}$  [2] ( $C_{3v}$  symmetry group), detected at  $850\text{ nm}$  in the gas phase by the author. In fact, their absorption bands in the infrared (IR) and in the near-infrared (NIR) part of the e.m. spectra are very similar.

Methyl iodide is a prolate symmetric top molecule, which is used in agriculture as a pesticide and is present in the earth's atmosphere, classified as halogenated volatile organic compound (HVOC). It participates to the ozone layer depletion [3]. This molecule is one of the most investigated in the IR, where it can be finely studied by spectroscopy based on semiconductor sources.

The  $\text{CH}_3\text{I}$  absorption spectrum between  $850\text{ nm}$  and  $2.5\text{ }\mu\text{m}$  has been detected in the distant past by Gehrard and Luise Herzberg [4] using an infrared prism spectrometer, when they classified the observed overtone and combination bands. Even older is the work of Verleger on methyl halides at wavelengths below  $1.2\text{ }\mu\text{m}$  [5], where overtone bands have been observed on photographic plates through a  $3\text{ m}$  grating monochromator. Methyl iodide optical absorption has been more recently studied in the NIR by Ishibashi and Sasada [6] with diode lasers as the sources to detect the  $2\nu_4$  overtone band at  $6,050\text{ cm}^{-1}$  with sub-Doppler resolution in a Fabry-Perot (F.-P.) type cavity measurement cell.

In this experimental work a tunable diode laser spectrometer (TDLS) with the frequency modulation and the second harmonic detection technique was used to observe the  $\text{CH}_3\text{I}$  ro-vibrational band at around  $11740\text{ cm}^{-1}$  ( $850\text{ nm}$ ) with a resolution of  $0.01\text{ cm}^{-1}$ . This NIR band is presumably related to the third overtone of the  $\nu_1$  quanta of C-H stretching excitation [4] or a combination of overtones, such as, for instance,  $2\nu_1 + 2\nu_4$ . This can lead to overlapping absorption bands, whose upper states can be coupled through Fermi and Coriolis resonances [7]. Therefore it is difficult to identify the right

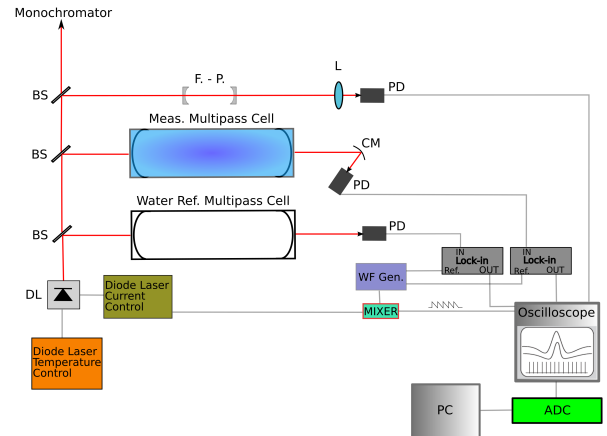


FIG. 1. Outline of the experimental apparatus. ADC: analog-to-digital converter; BS: beam splitter; CM: concave mirror; DL: diode laser; F. - P.: confocal Fabry-Perot interferometer; L: lens; PC: desk-top computer; PD: photodiode; WF Gen.: waveform generator.

ro-vibrational quanta, unless sophisticated techniques are employed, such as for example microwave-optical double resonance [8].

This absorption band is very weak, as the dipole moment is even less than the one of  $\text{CH}_3\text{F}$  and  $\text{CH}_3\text{Cl}$ , as the C-I bond length is shorter the C-F and C-Cl ones, therefore lower absorption strength for this molecule is expected. It is therefore necessary to use long optical paths and noise reduction techniques to observe and study these absorption lines.

Frequency Modulation Spectroscopy (FMS) [9], conventionally called Wavelength Modulation Spectroscopy (WMS) when the modulation frequency is much lower than the sampled line-width, was used on this occasion as a noise-reduction technique.

\* lucchesini@ino.cnr.it

## II. EXPERIMENT

### A. Experimental setup

The schematic of the experimental apparatus is illustrated in Fig. 1 and follows the previous work on  $\text{CH}_3\text{Cl}$  [2]. The employed source was the single mode Al-GaAs/GaAs double heterostructure F-P type diode laser (DL), Thorlabs L852P100, with maximum power  $\simeq 100$  mW cw in *free-running* configuration.

The DL temperature control is very critical as its typical emission wavelength varies as about 0.1 nm/K, therefore a customized bipolar temperature controller was adopted to drive a Peltier junction coupled to the DL mount. This guaranteed a stability of  $\sim 0.002$  K per hour. Also the DL current needs precise and fine control, since the characteristic slope of the DL emission is about 0.01 nm/mA. Consequently a low noise DL current controller was needed: for this experiment a custom-made current source was used, operating between 0 and 250 mA, with an accuracy of  $\pm 2.5$   $\mu\text{A}$ . To modulate and sweep the emission source, a sine wave carrier from a low noise waveform generator was mixed with the ramp extracted from the oscilloscope sawtooth signal and then sent to the DL current controller.

Two custom Herriott-type astigmatic multipass cells with optical path lengths of 30 m were used to house the sample and reference gases. The latter contained water vapor at room temperature (RT) with a partial pressure  $\simeq 20$  torr and was used as the reference gas for wavenumber measurements (for this purpose, the HITRAN2016 molecular spectroscopic database [10] was adopted) and to verify whether the water absorption lines could interfere with the observed  $\text{CH}_3\text{I}$  lines. At the exit of the measurement cell, a concave mirror focused the laser beam on the active spot of the photodiode (PD), with the purpose of reducing the mechanical noise coming from the optical leverage of the spectroscopy set.

Pre-amplified silicon PDs (Centronic OSD5-5T, with active surface of 2.52 mm diameter) were used as detectors, whose outputs were sent to lock-in amplifiers tuned to the carrier frequency ( $f \sim 5$  kHz) coming from the waveform generator. It was verified that the residual phase errors in the synchronization of the two lock-in amplifiers could induce at most a corresponding wavenumber error of  $0.003$   $\text{cm}^{-1}$ . A confocal 5 cm F.-P. interferometer (f.s.r. =  $0.05$   $\text{cm}^{-1}$ ) was utilized to check the DL emission mode and the linearity of its emission frequency, while a 35 cm focal length Czerny-Turner monochromator with 1,180 lines per mm grating was used for the rough wavelength check ( $\pm 0.01$  nm).

The vacuum in the sample cell was obtained by a double stage rotary pump with limit pressure  $< 1 \times 10^{-4}$  torr, and the pressure inside the cell was directly measured by a capacitive pressure gauge (accuracy  $\pm 0.5$  torr). All experiments were conducted at RT and at pressure values ranging from 20 to 90 torr. Analytical grade methyl iodide (Sigma-Aldrich, 99% purity, with silver as stabi-

lizer) was used as supplied. The sample was contained in a stainless steel tube and it was allowed to flow into the evacuated measuring cell at its vapor pressure.

### B. Wavelength Modulation Spectroscopy

The transmittance  $\tau(\nu)$  after the sampled gas can be described by the Lambert-Beer expression:

$$\tau(\nu) = e^{-\sigma(\nu)z} \quad (1)$$

where  $z = \rho l$  is the product of the absorbing species density  $\rho$  (molecule/ $\text{cm}^3$ ) and the optical path  $l$  (cm) of the radiation through the sample, namely the *column amount* (molecule/ $\text{cm}^2$ ), and  $\sigma(\nu)$  is the absorption cross-section ( $\text{cm}^2/\text{molecule}$ ), which follows the line-shape behaviour, but in regimes of small optical depth [ $\sigma(\nu)z \ll 1$ ] as in most experimental conditions, Eq. (1) can be approximated by

$$\tau(\nu) \simeq 1 - \sigma(\nu)z. \quad (2)$$

The WMS technique was achieved here by modulating the the source emission frequency  $\bar{\nu}$  at  $\nu_m = \omega_m/2\pi$ , with amplitude  $a$ :

$$\nu = \bar{\nu} + a \cos \omega_m t. \quad (3)$$

The transmitted intensity could then be written as a cosine Fourier series:

$$\tau(\bar{\nu} + a \cos \omega_m t) = \sum_{n=0}^{\infty} H_n(\bar{\nu}, a) \cos n\omega_m t \quad (4)$$

where  $H_n(\bar{\nu})$  is the  $n$ -th harmonic component of the modulated signal. With a lock-in amplifier tuned to a multiple  $n\nu_m$  ( $n = 1, 2, \dots$ ) of the modulation frequency, an output signal proportional to the  $n$ -th component  $H_n(\bar{\nu})$  is obtained. In case the value of  $a$  is chosen smaller than the line-width, the  $n$ -th Fourier component is proportional to the  $n$ -th derivative of the original signal:

$$H_n(\bar{\nu}, a) = \frac{2^{1-n}}{n!} a^n \left. \frac{d^n \tau(\nu)}{d\nu^n} \right|_{\nu=\bar{\nu}}, \quad n \geq 1. \quad (5)$$

In order to detect very low absorbances, a high modulation amplitude regime is required, which implies a modulation index  $m \equiv a/\Gamma \gg 0.1$ , where  $\Gamma$  is the absorption line-width.

Line position measurements were carried on at pressures around 30 torr. In this condition, where the collisional effect was not negligible, the absorption line shape was well described by the Voigt profile, a convolution of the Gaussian (Doppler regime) and Lorentzian (collisional regime) functions:

$$f(\nu) = \int_{-\infty}^{+\infty} \frac{\exp[-(t - \nu_0)^2/\Gamma_G^2 \ln 2]}{(t - \nu)^2 + \Gamma_L^2} dt \quad (6)$$

where  $\nu_0$  is the gas resonance frequency,  $\Gamma_G$  and  $\Gamma_L$  are the Gaussian and the Lorentzian half-widths at half-the-maximum (HWHM), respectively. Second-order effects, such as speed-changing collision or Dicke narrowing [11], were not observed within the sensitivity of the apparatus and therefore were not taken into account.

The phase detection technique, obtained by tuning the lock-in amplifiers to twice the modulation frequency ( $\sim 10$  kHz), produced a line-shape signal that was closer to the 2nd derivative of the absorption feature as the minor was the amplitude of the modulation. The symmetry of the line shape was not perfect due to the simultaneous amplitude modulation of the source signal as the injection current of the diode laser varied; indeed, this effect becomes negligible in high modulation regimes. Such “ $2f$  detection” has the advantage of a flat baseline of the signal, but cannot avoid optical interferences, coming from the many reflecting surfaces present in the optical path. This is the main drawback of this spectroscopic technique, which in the specific case has limited the detection sensitivity to absorbances higher than  $1 \times 10^{-7}$ . Under these conditions this technique could not provide a reliable measurement of the intensity parameter when applied to very weak resonances. For this reason it was possible only to estimate that the strength of the  $\text{CH}_3\text{I}$  absorption lines here lies in the interval  $1 - 30 \times 10^{-27}$  cm/molecule from a comparison with the absorption line strengths of the water vapor present in the same spectrum, centered around  $11740 \text{ cm}^{-1}$ , where the strongest lines were found.

To obtain line positions and widths with good reliability even for the weakest lines, the values of the modulation index  $m$  have been set around 2.0–2.3. This substantially improved the S/N ratio, but did not allow the use of Eq. (5) any more. The approximate function that represents the absorption line distorted by the modulation has been specifically evaluated and is reported in the Appendix; a nonlinear least-squares fit method was applied to extract line parameters from the collected profiles.

Finally, the following expression of the collisional half-width at half-maximum (HWHM) as a function of pressure was adopted for the line broadening calculations:

$$\Gamma_L(p) = \gamma_{\text{self}} p \quad (7)$$

where  $p$  is the sample gas pressure, and  $\gamma_{\text{self}}$  is the gas self-broadening coefficient.

### III. EXPERIMENTAL RESULTS

The 82  $\text{CH}_3\text{I}$  absorption lines have been detected and are listed in Table I, where the maximum error on the wavenumber ( $\nu'$ ) was within the second decimal unit, referring to the ten times more precise  $\text{H}_2\text{O}$  atlas [10]. The wavelengths are reported for convenience in air at  $T = 294$  K, following the work of Edlén [12].

Fig. 2 presents the  $2f$  absorption measurement signal for  $\text{CH}_3\text{I}$  at  $11789.28 \text{ cm}^{-1}$ ,  $T = 294$  K,  $p_{\text{CH}_3\text{I}} = 31$  torr,

TABLE I. Wavenumbers and wavelengths (in air at room temperature) of the detected  $\text{CH}_3\text{I}$  absorption lines, with the maximum error within the second decimal unit.

$\nu'$ ( $\text{cm}^{-1}$ )	$\lambda$ ( $\text{\AA}$ )	$\nu'$ ( $\text{cm}^{-1}$ )	$\lambda$ ( $\text{\AA}$ )
11659.92	8574.08	11697.76	8546.35
11660.13	8573.93	11698.02	8546.16
11664.91	8570.41	11700.55	8544.31
11665.03	8570.33	11700.85	8544.09
11667.27	8568.68	11700.95	8544.02
11683.78	8556.57	11704.88	8541.15
11683.92	8556.47	11706.39	8540.04
11684.03	8556.39	11706.48	8539.98
11684.18	8556.28	11706.55	8539.94
11684.43	8556.10	11706.77	8539.77
11684.58	8555.99	11709.79	8537.57
11684.74	8555.87	11709.94	8537.46
11684.95	8555.41	11710.29	8537.20
11686.83	8554.34	11710.55	8537.01
11687.14	8554.11	11711.17	8536.56
11687.44	8553.89	11711.41	8536.38
11687.72	8553.69	11711.53	8536.30
11694.13	8549.00	11711.64	8536.22
11694.39	8548.81	11713.72	8534.70
11694.67	8548.61	11713.81	8534.64
11697.42	8546.59	11720.67	8529.65

TABLE I. Wavenumbers and wavelengths of the detected  $\text{CH}_3\text{I}$  absorption lines (continued).

$\nu'$ ( $\text{cm}^{-1}$ )	$\lambda$ ( $\text{\AA}$ )	$\nu'$ ( $\text{cm}^{-1}$ )	$\lambda$ ( $\text{\AA}$ )
11720.95	8529.44	11770.45	8493.57
11730.12	8522.77	11772.70	8491.94
11730.34	8522.61	11777.29	8488.63
11730.43	8522.54	11777.94	8488.17
11730.62	8522.41	11778.05	8488.09
11738.96	8516.35	11778.27	8487.93
11739.46	8515.99	11785.46	8482.75
11739.58	8515.90	11785.65	8482.61
11739.69	8515.82	11786.01	8482.35
11739.80	8515.74	11788.60	8480.49
11741.14	8514.77	11789.28	8480.00
11741.39	8514.59	11798.00	8473.73
11748.32	8509.57	11805.97	8468.01
11761.04	8500.36	11806.13	8467.90
11761.75	8499.85	11826.25	8453.49
11767.15	8495.95	11827.97	8452.26
11767.29	8495.85	11841.21	8442.81
11767.42	8495.75	11841.39	8442.68
11768.03	8495.31	11841.46	8442.63
11768.13	8495.24	11842.02	8442.23

and  $m \simeq 2$ , along with the best fit and its residuals. It displays also the  $\text{H}_2\text{O}$   $2f$  reference signal at  $11789.41 \text{ cm}^{-1}$  and the transmission of the F.-P. interferometer used for frequency linearization. The evident etalon effect in the  $\text{CH}_3\text{I}$  measurement plot originates from reflections within the optical path, and it has been taken into account in the fit procedure. Only the higher frequency

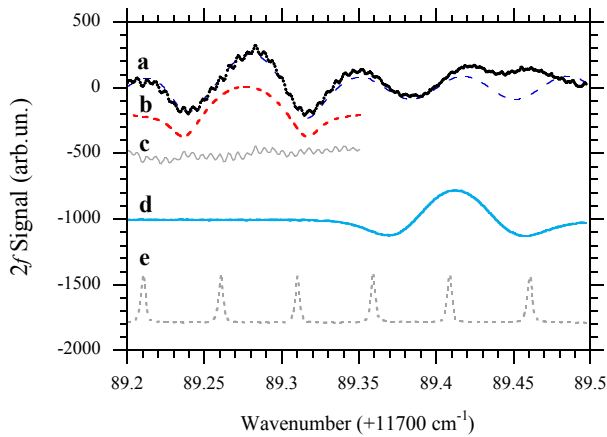


FIG. 2. 2nd harmonic absorption signal of  $\text{CH}_3\text{I}$  around 848 nm (black dots) at  $p = 31$  torr and RT, with the best fit (dashed blue line) (a), the extracted peak fit (b) and the residuals (c), along with the  $\text{H}_2\text{O}$  reference signal (d), all obtained by WMS with 10 Hz bandwidth. The F.-P. interferometer transmission (f.s.r.=  $0.05 \text{ cm}^{-1}$ ) is also shown (e).

TABLE II. Measured  $\text{CH}_3\text{I}$  HWHM self-broadening coefficients.

$\nu'$ ( $\text{cm}^{-1}$ )	$\gamma_{\text{self}}$ ( $\text{cm}^{-1}/\text{atm}$ )
11741.39	$0.23 \pm 0.02$
11778.27	$0.18 \pm 0.02$

fringes remain in the fit residuals, originating from the confocal mirrors of the multipass cell; in fact the distance between them is  $l = 42.8 \text{ cm}$  and  $\Delta\nu' \cong 1/(4l) = 0.0058 \text{ cm}^{-1}$ .

The self-broadening coefficients ( $\gamma_{\text{self}}$ ) were measured for the first time for two  $\text{CH}_3\text{I}$  lines at RT and are shown in Table II. Fig. 3 shows the self-broadening measurement result for the line at  $11741.39 \text{ cm}^{-1}$ , where the Lorentzian component of the absorption line-width is plotted as a function of methyl iodide pressure at RT.

In the literature, we did not find any measurements of pressure line-broadening at these wavenumbers, but a comparison can be attempted with what was obtained in other spectral regions.

In HITRAN database [10] for the  $\nu_4$  fundamental band at  $3.3 \mu\text{m}$  the  $\gamma_{\text{self}}$  is reported between  $0.1$  a  $0.5 \text{ cm}^{-1}/\text{atm}$  at  $296 \text{ K}$ . K.J. Hoffman et al. [13] by diode laser absorption spectroscopy observed  $\gamma_{\text{self}}$  at RT for the  $\nu_5$  band at  $7 \mu\text{m}$  from  $0.10$  to  $0.45 \text{ cm}^{-1}/\text{atm}$ . Rad-daoui et al. [14] by a Fourier transform spectrometer at RT obtained  $\gamma_{\text{self}}$  ranging from  $0.10 \text{ cm}^{-1}/\text{atm}$  (at low and high quantum rotational parameter  $J$ ) and  $0.45 \text{ cm}^{-1}/\text{atm}$  for the  $\nu_6$  fundamental roto-vibrational band of  $\text{CH}_3\text{I}$  at around  $11 \mu\text{m}$ . Again, in this ro-vibrational band at RT, Attafi et al. [15] obtained  $\gamma_{\text{self}}$  from  $0.15$  to

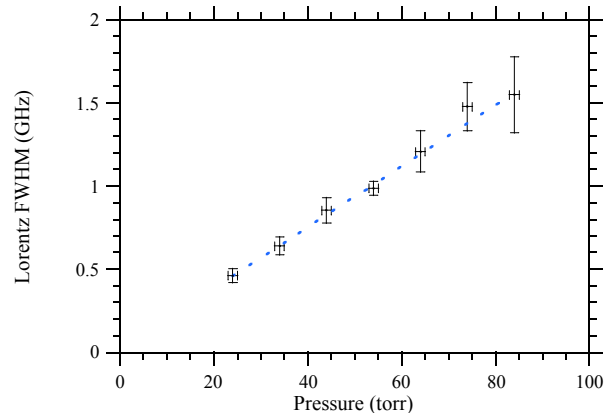


FIG. 3. Self-broadening measurements on the methyl iodide  $11741.39 \text{ cm}^{-1}$  absorption line at RT obtained by TDLS and the procedure explained in the text. The blue dashed line shows the best linear fit.

$0.36 \text{ cm}^{-1}/\text{atm}$ . Belli et al. [16] with the Doppler-free double-resonance technique have got the self collisional broadening parameters at RT for some absorption lines in the  $\nu_6$  fundamental band, presenting values ranging from  $0.18$  to  $0.20 \text{ cm}^{-1}/\text{atm}$ . Finally Ben Fathallah et al. using Fourier transform spectroscopy at RT obtained self-broadening coefficient values from  $0.14$  to  $0.36 \text{ cm}^{-1}/\text{atm}$  for the bands  $\nu_5$  and  $\nu_3 + \nu_6$  [17], while for the band  $\nu_2$  [18] at around  $8 \mu\text{m}$  they obtained an average value of  $\gamma_{\text{self}}$  equal to  $0.25 \text{ cm}^{-1}/\text{atm}$ , with a minimum at  $0.1 \text{ cm}^{-1}/\text{atm}$  and a maximum at  $0.4 \text{ cm}^{-1}/\text{atm}$ .

Our results are within all of this ranges.

#### IV. CONCLUSION

82 new  $\text{CH}_3\text{I}$  absorption lines between  $11660$  and  $11840 \text{ cm}^{-1}$  have been measured for the first time with a precision of  $0.01 \text{ cm}^{-1}$ , using a tunable diode laser spectrometer, the wavelength modulation spectroscopy, and the second harmonic detection in a 30 m Herriott-type multipass cell. A high modulation amplitude approach was adopted, and a dedicated fit function was developed. The strength of the observed lines varied between  $10^{-27}$  and  $10^{-26} \text{ cm}^2/\text{molecule}$  at room temperature. For two of the observed lines, self-broadening coefficients similar to those reported for the same molecule in other spectral regions were obtained for the first time.

#### V. ACKNOWLEDGMENTS

Thanks are due to A. Barbini for the electronic consultancy, to M. Tagliaferri and to M. Voliani for the technical assistance. The author is indebted to D. Bertolini for the calculations in the high modulation approximation.

### Appendix: Frequency modulation in the high amplitude regime

The use of high modulation amplitude  $a$  is a necessity in order to increase the S/N ratio for very weak absorption lines. In this case the derivative approximation of Eq. (5) no longer works and it is more appropriate to start from the other expression [19]:

$$H_n(\nu, a) = \frac{2}{\pi} \int_0^\pi \tau(\nu + a \cos \theta) \cos n\theta \, d\theta. \quad (\text{A.1})$$

In order to extract the collisional component from the absorption line-shape, Arndt [20] and Wahlquist [21] derived the analytic form of the harmonics for a Lorentzian function, which is the right choice when dealing with collisional broadening.

To do this they obtained the  $n$ th harmonic element in-

---


$$H_2(x, m) = \frac{2}{m^2} - \frac{2^{1/2}}{m^2} \times \frac{1/2[(M^2 + 4x^2)^{1/2} + 1 - x^2][(M^2 + 4x^2)^{1/2} + M]^{1/2} + |x|[(M^2 + 4x^2)^{1/2} - M]^{1/2}}{(M^2 + 4x^2)^{1/2}} \quad (\text{A.6})$$

where

$$M = 1 - x^2 + m^2.$$

Eq. (A.6), close to the second derivative of the absorption feature only for low  $m$ , simulates the behavior of the

verting Eq. (4):

$$H_n(x, m) = \varepsilon_n i^n \int_{-\infty}^{+\infty} \hat{\tau}(\omega) J_n(m\omega) e^{i\omega x} \, d\omega \quad (\text{A.2})$$

where

$$\hat{\tau}(\omega) = \frac{1}{2\pi} \int \tau(x) e^{-i\omega x} \, dx \quad (\text{A.3})$$

is the Fourier transform of the transmittance profile;  $x = \nu/\Gamma$  and  $m = a/\Gamma$ ,  $\Gamma$  is the line-width;  $J_n$  is the  $n$ th order Bessel function;  $\varepsilon_0 = 1$ ,  $\varepsilon_n = 2$  ( $n = 1, 2, \dots$ ) and  $i$  is the imaginary unit. The absorption cross-section in Eq. (2) is then put in the Lorentzian form:

$$\sigma_L(x, m) \propto \frac{1}{1 + (x + m \cos \omega t)^2}. \quad (\text{A.4})$$

The second Fourier component of the absorption cross section can be recalculated following Arndt's work by setting  $n = 2$ :

$$H_2(x, m) = -\frac{1}{m^2} \left[ \frac{\{[(1 - ix)^2 + m^2]^{1/2} - (1 - ix)\}^2}{[(1 - ix)^2 + m^2]^{1/2}} + \text{c.c.} \right] \quad (\text{A.5})$$

and by eliminating the imaginary part:

---

line-shape at high modulation amplitudes. This is shown in Fig. 4, where the equation is plotted in 3D, varying the modulation index  $m$ . For  $m = 3$  the 2nd derivative is completely deformed by broadening, as it happens in reality.

- 
- [1] A. Lucchesini and S. Gozzini, Diode laser spectroscopy of methyl fluoride overtones at 850 nm, *J. Quant. Spectrosc. Radiat. Transfer.* **130**, 352 (2013), HITRAN2012 Special Issue.
  - [2] A. Lucchesini and S. Gozzini, Diode laser spectroscopy of methyl chloride overtones at 850–860nm, *J. Quant. Spectrosc. Radiat. Transfer.* **168**, 170 (2016).
  - [3] J. C. Laube, S. Tegtmeier, R. P. Fernandez, J. Harrison, L. Hu, P. Krummel, E. Mahieu, S. Park, and L. Western, Update on ozone-depleting substances (odss) and other gases of interest to the Montreal protocol, in *Scientific Assessment of Ozone Depletion: 2022*, edited by W.M.O (Geneva, Switzerland, 2022) Chap. 1, pp. 55–113.
  - [4] G. Herzberg and L. Herzberg, Absorption spectrum of methyl iodide in the near infrared, *Can. J. of Res.* **27b**, 332 (1949).
  - [5] H. Verleger, Das rotationsschwingungsspektrum der methylhalogenide im photographischen ultrarot bei 1.11  $\mu\text{m}$ , *Z. Physik* **98**, 342 (1935).
  - [6] C. Ishibashi and H. Sasada, Near-infrared laser spectrometer with sub-doppler resolution, high sensitivity, and wide tunability: A case study in the 1.65- $\mu\text{m}$  region of  $\text{CH}_3\text{I}$  spectrum, *J. Mol. Spectrosc.* **200**, 147 (2000).
  - [7] M. M. Law, Joint local- and normal-mode studies of the overtone spectra of the methyl halides:  $\text{CH}_3\text{F}$ ,  $\text{CH}_3\text{Cl}$ ,  $\text{CH}_3\text{Br}$ ,  $\text{CD}_3\text{Br}$ , and  $\text{CH}_3\text{I}$ , *J. Chem. Phys.* **111**, 10021 (1999).
  - [8] C. Ishibashi, R. Saneto, and H. Sasada, Infrared radio-frequency double-resonance spectroscopy of molecular

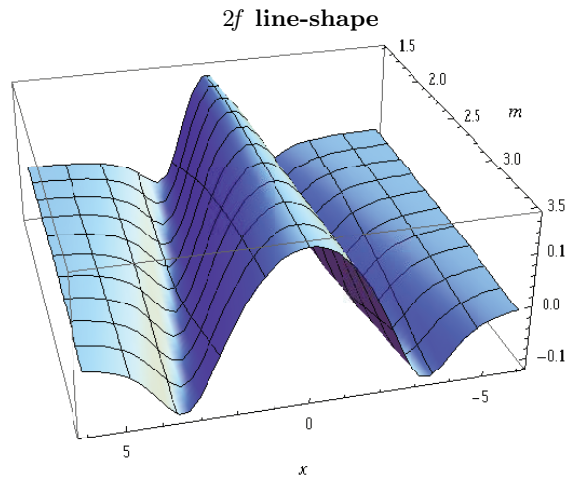


FIG. 4. Behavior of Eq. (A.6) as a function of the modulation parameter  $m$ .

vibrational-overtone bands using a Fabry–Perot cavity-absorption cell, *J. Opt. Soc. Am. B* **18**, 1019 (2001).

- [9] G. C. Bjorklund, Frequency-modulation spectroscopy: a new method for measuring weak absorptions and dispersions, *Opt. Lett.* **25**, 15 (1980).
- [10] I. E. Gordon, L. S. Rothman, C. Hill, R. V. Kochanov, Y. Tan, P. F. Bernath, M. Birk, V. Boudon, A. Campargue, K. V. Chance, and et al., The HITRAN 2016 molecular spectroscopic database, *J. Quant. Spectrosc. Radiat. Transfer.* **203**, 3 (2017), HITRAN2016 Special Issue.
- [11] R. H. Dicke, The effect of collision upon the doppler width of the spectral lines, *Phys. Rev.* **89**, 472 (1953).
- [12] B. Edlén, The refractive index of air, *Metrol.* **2**, 71 (1966).
- [13] K. J. Hoffman and P. B. Davies, Pressure broadening coefficients of  $\nu_5$  fundamental band lines of  $\text{CH}_3\text{I}$  at  $7\ \mu\text{m}$  measured by diode laser absorption spectroscopy, *J. Mol. Spectrosc.* **252**, 101 (2008).
- [14] E. Raddaoui, L. Troitsyna, A. Dudaryonok, P. Soulard, M. Guinet, H. Aroui, J. Buldyreva, N. Lavrentieva, and D. Jacquemart, Line parameters measurements and modeling for the  $\nu_6$  band of  $\text{CH}_3\text{I}$ : A complete line list for atmospheric databases, *J. Quant. Spectrosc. Radiat. Transfer.* **232**, 165 (2019).
- [15] Y. Attafi, A. Ben Hassen, H. Aroui, F. Kwabia Tchana, L. Manceron, D. Doizi, J. Vander Auwera, and A. Perrin, Self and  $\text{N}_2$  collisional broadening of rovibrational lines in the  $\nu_6$  band of methyl iodide ( $^{12}\text{CH}_3\text{I}$ ) at room temperature: The  $J$  and  $K$  dependence, *J. Quant. Spectrosc. Radiat. Transfer.* **231**, 1 (2019).
- [16] S. Belli, G. Buffa, A. Di Lieto, P. Minguzzi, O. Tarrini, and M. Tonelli, Hyperfine level dependence of the pressure broadening of  $\text{CH}_3\text{I}$  rotational transitions in the  $\nu_6 = 1$  vibrational state, *J. Mol. Spectrosc.* **201**, 314 (1980).
- [17] O. Ben Fathallah, F. Hmida, A. Boughdiri, L. Manceron, M. Rotger, and H. Aroui, Line intensities and self-broadening coefficients of  $\text{CH}_3\text{I}$  in the region of  $\nu_5$  and  $\nu_3 + \nu_6$  bands, *J. Quant. Spectrosc. Radiat. Transfer.* **275**, 107893 (2021).
- [18] O. Ben Fathallah, W. Hammi, A. Boughdiri, L. Manceron, and H. Aroui, Measurements of line intensities and self-broadening coefficients in the  $\nu_2$  band of  $\text{CH}_3\text{I}$ , *J. Quant. Spectrosc. Radiat. Transfer.* **259**, 107449 (2021).
- [19] C. R. Webster, R. T. Menzies, and E. D. Hinkley, Infrared laser absorption: Theory and applications, in *Laser Remote Chemical Analysis*, edited by R. M. Measures (John Wiley & Sons, Ltd, New York, NY, 1988).
- [20] R. Arndt, Analytical line shapes for lorentzian signals broadened by modulation, *J. Appl. Phys.* **36**, 2522 (1965).
- [21] H. Wahlquist, Modulation broadening of unsaturated lorentzian lines, *J. Chem. Phys. B* **35**, 1708 (1961).